The Impact of Land Cover Change on a Simulated Storm Event in the Sydney Basin

A. F. GERO AND A. J. PITMAN

Department of Physical Geography, Macquarie University, Sydney, New South Wales, Australia

(Manuscript received 21 March 2005, in final form 2 August 2005)

ABSTRACT

The Regional Atmospheric Modeling System (RAMS) was run at a 1-km grid spacing over the Sydney basin in Australia to assess the impact of land cover change on a simulated storm event. The simulated storm used NCEP–NCAR reanalysis data, first with natural (i.e., pre-European settlement in 1788) land cover and then with satellite-derived land cover representing Sydney's current land use pattern. An intense convective storm develops in the model in close proximity to Sydney's dense urban central business district under current land cover. The storm is absent under natural land cover conditions. A detailed investigation of why the change in land cover generates a storm was performed using factorial analysis, which revealed the storm to be sensitive to the presence of agricultural land in the southwest of the domain. This area interacts with the sea breeze and affects the horizontal divergence and moisture convergence—the triggering mechanisms of the storm. The existence of the storm over the dense urban area of Sydney is therefore coincidental. The results herein support efforts to develop parameterization of urban surfaces in high-resolution simulations of Sydney's meteorological environment but also highlight the need to improve the parameterization of other types of land cover change at the periphery of the urban area, given that these types dominate the explanation of the results.

1. Introduction

Land surface processes affect weather through the exchange of heat, moisture, and momentum between the earth's surface and the atmosphere (Betts et al. 1996). Studies by Beljaars et al. (1996) and Viterbo and Betts (1999) of the July 1993 floods in the United States showed that the simulation of precipitation by the European Centre for Medium-Range Weather Forecasts was highly sensitive to the parameterization of surface processes. Soil moisture anomalies (Schar et al. 1999), soil freezing (Viterbo et al. 1999), surface parameters and aggregating functions (Rodriguez-Camino and Avissar 1999), land surface heterogeneity (Avissar and Pielke 1989; Holtslag and Ek 1995), and the nature of the vegetation (Pielke et al. 1997) have all been shown to affect various aspects of the boundary layer and its meteorological components (see Avissar et al. 2004).

Many studies have shown urban surfaces to be capable of altering natural weather patterns through the urban heat island effect, the disruption of airflow, and the initiation of mesoscale circulations, and by affecting storm occurrence. For example, in an early modeling study, Hjelmfelt (1982) demonstrated that wind flow can be altered by an urban surface. A more recent study by Kalnay and Cai (2003) focused on the thermal impacts of urbanization [there is significant dispute over their results, however; see Trenberth (2004)]. Numerous other modeling studies have been undertaken to investigate the effect of urban surfaces on weather and climate, facilitated by improved knowledge of physical processes coupled with enhanced computing capacity. Thorough reviews of the urban influence on climate are found in Pielke (2001) and Arnfield (2003). More specific storm studies, including Atkinson (1971), Balling and Brazel (1987), Jauregui and Romales (1996), Bornstein and Lin (2000), and Baik et al. (2001), demonstrate how urban areas can affect storm initiation, intensity, and motion.

Observational evidence also suggests an urban influence on weather and climate. Some studies find increases in warm-season rainfall downwind of cities (e.g., Changnon 1968; Landsberg 1970; Huff 1986). There is also evidence for cities causing decreased precipitation amounts by altering cloud microphysics

Corresponding author address: Professor A. J. Pitman, Department of Physical Geography, Macquarie University, North Ryde, NSW 2109, Australia.
E-mail: apitman@els.mq.edu.au

(Rosenfield 1999; Ramanathan et al. 2001). An observational study by Shepherd and Burian (2003) notes the significance of the sea breeze and coastline curvature in addition to the city surface in contributing to the meteorological conditions of coastal cities, highlighting some of the complexities in urban–atmosphere studies. Evidence local to Sydney, Australia, supports both the potential role of the sea breeze in enhancing storm frequency (see Potts et al. 2000) and sea breezes as a form of boundary layer convergence that initiates convection [this has been found in earlier studies, including Wilson and Schreiber (1986) and Koch and Ray (1997)]. Overall, the specific physical setting of cities are important in determining meteorological outcomes, and generalized assessments of urban influences on weather and climate must be reviewed critically (Shepherd and Burian 2003).

This paper focuses on the Sydney basin and explores the impact of land cover change (LCC) on a single storm event occurring in the region. At first, LCC within the Sydney basin was to support agriculture, but recent urban expansion in the Sydney region has been extensive to accommodate an influx of 50 000 people per year (Environmental Protection Authority, New South Wales 2003). The Sydney basin is frequently affected by storms, predominantly in summer during the early afternoon and evening (Potts et al. 2000). Case studies of several of Sydney's severe storms can be found in Spillane and Dixon (1969) and Bureau of Meteorology (1993, 1995), and Matthews and Geerts (1995) provide a study of the spatial distribution of Sydney's storms according to synoptic type. The possible interaction of these storms with Sydney's urban surface is a growing concern as urbanization spreads, potentially exerting an increasing influence on the characteristics of severe storms. Given that the Sydney hailstorm of April 1999 caused the most insured damage of any natural disaster recorded in Australia (exceeding Australian $1.7 billion; see http://www.idro.com.au), any role of the land surface in intensifying or changing the frequency or timing of intense storms is worthy of study because it affects the exposure of the insurance industry to financial risk.

In this paper we explore a particularly interesting simulated storm. This storm did not occur in the model under natural land cover (land cover representing pre-European settlement that occurred in 1788) and only occurred under land cover patterns that now exist within the Sydney basin. We explore how the change in land cover affects the thermodynamic conditions that contribute to the storm and maintain it. To assess the influence of the particular landscape pattern across the Sydney basin, a factorial assessment of the sensitivity of the storm to the pattern of land cover was performed. The details of the high-resolution numerical model used to simulate the storm are provided in section 2. Section 3 describes and discusses the results. Section 4 presents a summary and conclusions.

2. Model description and experimental method

This study used the Regional Atmospheric Modeling System (RAMS; version 4.3.0). RAMS implements the fundamental equations of heat, moisture, momentum, and continuity (Pielke 2001), and was described in detail by Pielke et al. (1992) and Cotton et al. (2003). The model has been used extensively across a range of applications, including in an operational capacity (e.g., McQueen et al. 1999; Aikman et al. 2000). The pertinent features of the model configuration used in this study are presented in Table 1. The model configuration was selected based on the desire to capture both the small-scale convective processes and the larger mesoscale and synoptic-scale processes that contribute to storm occurrence. For further detail on each of the parameterization schemes, readers are referred to literature cited in Table 1.

For this study, four nested grids with horizontal grid

TABLE 1. Summary of model configuration used in this study.

Grid nesting structure	Four grids of 1-, 3-, 12-, and 60-km horizontal grid spacing, following Pielke et al. (1997)
Initialization method	Horizontally heterogeneous using NCEP–NCAR reanalysis (Kalnay et al. 1996), following Narisma and Pitman (2003) and Peel et al. (2005)
Lateral boundary conditions	Klemp and Wilhelmson (1978), following Walko and Tremback (2002)
Cumulus parameterization	Kain and Fritsch (1993) for grids 1 and 2 and none for grids 3 and 4, following Castro et al. (2001) [note that Kain and Fritsch (1993), when used with a 60-km grid, is not generally recommended; we found it superior to Kuo (1974) as modified by Tremback (1990) in these specific experiments but advise caution in its use generally at this grid spacing]
Radiative transfer	Harrington (1997), following Walko et al. (1995) and Pielke (2001)
Microphysics	Level 3, bulk microphysics (see Meyers et al. 1992), following Cotton et al. (1995)
Land surface model	LEAF-2 (Walko et al. 2000), following many RAMS studies: e.g., Copeland et al. (1996), Pielke et al. (1997), and Rozoff et al. (2003)

TABLE 2. Grid configuration. The vertical spacing is constant for all grids, with 1.16 grid stretch ratio.

Grid No.	No. of horizontal grid points	Horizontal domain size (km)	Horizontal grid increment (km)	Time step (s)	Depth (m)	Vertical spacing (m)
1	50 × 50	2940 × 2940	60	120	24 860	100–1500
2	42 × 42	492 × 492	12	24	24 860	
3	50 × 50	147 × 147	3	6	17 360	
4	92 × 92	91 × 91	1	2	9860	

increments of 60, 12, 3and 1 km, respectively, were used (Table 2). This configuration has a relatively low nesting ratio and was chosen to improve the exchange of data between grids (Walko et al. 1995). Use of larger-spatial-resolution jumps between grids is more computationally efficient, but it can affect reliability and accuracy (Denis et al. 2003). Figure 1 shows the nested grid configuration and topography, and Fig. 2 shows the specific land cover classes for the fine grid (grid 4). Lateral boundary conditions were taken from the National Centers for Environmental Prediction–National Center for Atmospheric Research (NCEP–NCAR) reanalysis data (Kalnay et al. 1996) [we obtained from the NCAR mass storage system the specific dataset NCEP–

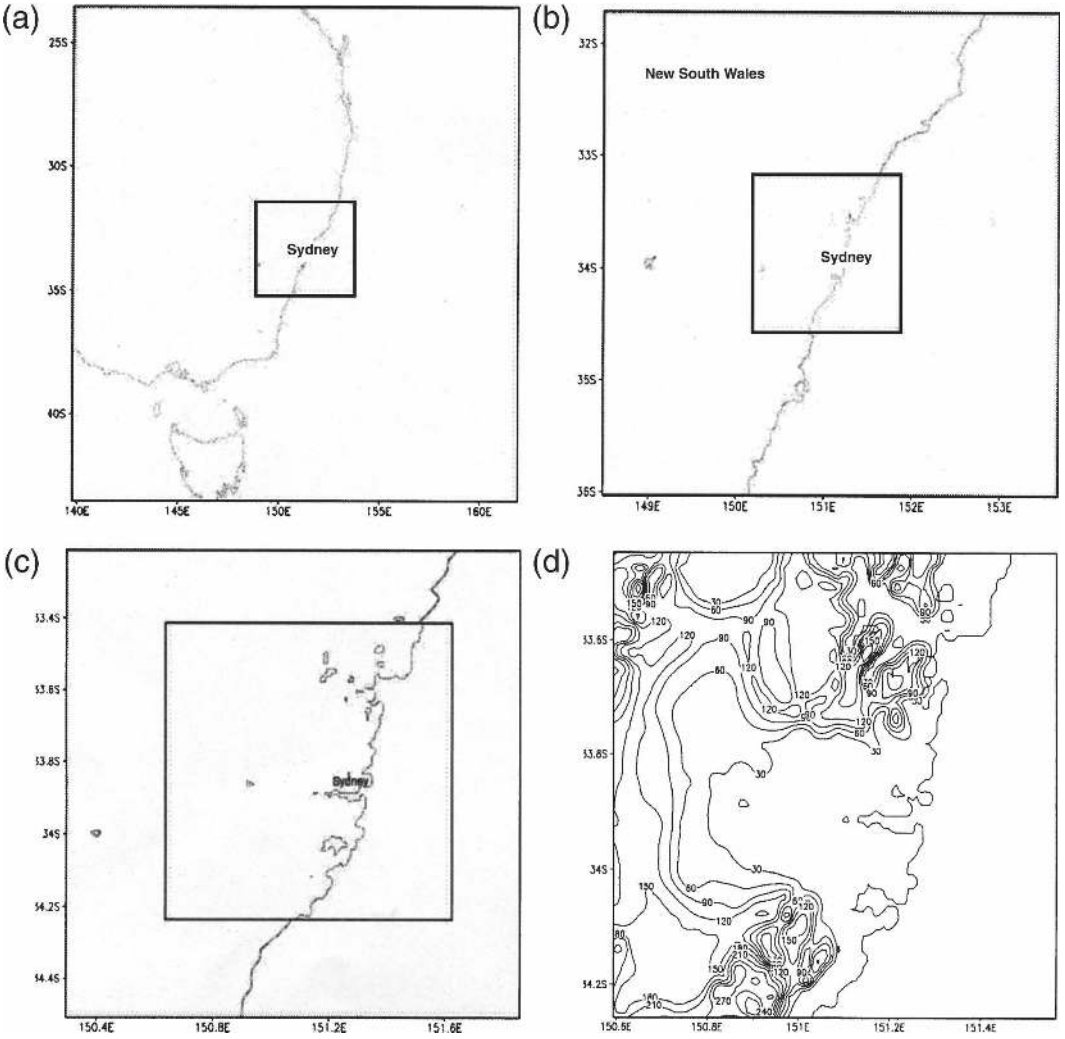

FIG. 1. Nesting structure of grids 1–4: (a) grid 1 with an inset of grid 2, (b) grid 2 with an inset of grid 3, (c) grid 3 with an inset of grid 4, and (d) grid 4 with topography (meters above sea level).

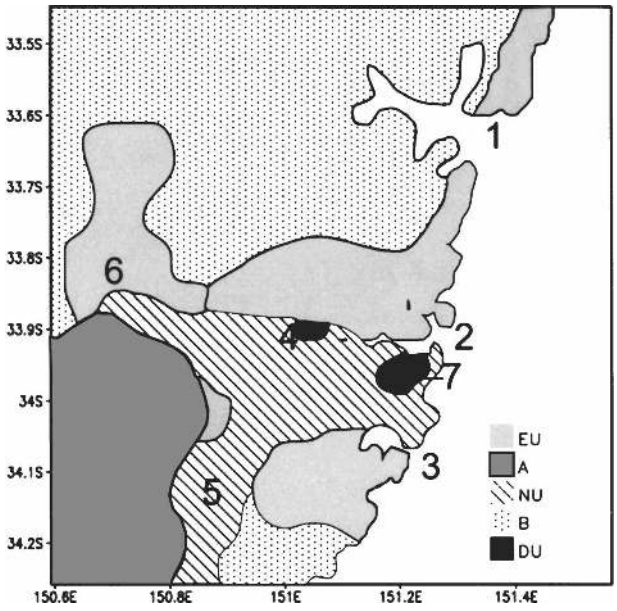

FIG. 2. Current land cover pattern for grid 4 (EU: established urban, A: agriculture, NU: new urban, B: bushland, and DU: dense urban; 1: Broken Bay, 2: Port Jackson, 3: Botany Bay, 4: Parramatta, 5: Campbelltown, and 6: Penrith).

NCAR Reanalysis 1: ds090.0]. These boundary conditions were updated every 6 h using the Klemp–Wilhelmson condition (Klemp and Wilhelmson 1978) based on results from Walko and Tremback (2002). Initialization for this study was horizontally inhomogeneous using data from the NCEP–NCAR reanalysis. Inhomogeneous initialization is commonly used in numerical weather prediction models in which observed temperature, winds, and humidities are incorporated (or assimilated) into a numerical model to provide the best spatial estimate of the initial atmospheric structure at each grid point and at each level in the atmosphere. Sea surface temperatures were initialized identically, using the same NCEP–NCAR data, at the beginning of each run, and, because we ran for single days, these temperatures were not updated. All of our simulations began at 1000 LST, which was several hours before the storm began to develop in the model. One issue with our model configuration is that the top of the atmosphere over grid 4 was limited to 9860 m. This height is very low but was retained to ensure consistency of the results with Gero et al. (2006). We tested the sensitivity of the results to deeper atmospheres using current and natural land cover, and our conclusions were not affected, but we did not repeat the factorial experiments with the deeper atmosphere.

The use of the NCEP–NCAR reanalysis has an important limitation for our study: it means that the storms simulated are not "real" in the sense that they can be compared with the observed meteorological conditions of a particular day. Over the data-rich United States it is possible that using this assimilation product would generate meteorological phenomena within RAMS that could be compared with observations, and a simulated storm could be validated against an observed storm. In more data-poor regions, such as Australia, we do not anticipate that the synoptic-scale NCEP–NCAR product accurately reflects the meteorological conditions over Sydney on a specific day, and therefore we do not expect a nested regional model such as RAMS to simulate accurately a specific storm that might have occurred on a specific day. Despite these apparent limitations we used the NCEP–NCAR data as lateral boundary conditions for a variety of reasons. We wanted the synoptic meteorological conditions to be physically reasonable over southwestern Australia (hence, we did not want to use synthetic or idealized conditions). Lateral boundary conditions from the Australia forecast system were incompatible with RAMS, leading to unresolved numerical instabilities in the model. Also, the NCEP–NCAR data were available and well documented, which is something of a luxury for research groups outside Europe and the United States.

To represent the land surface in RAMS, the Land Ecosystem–Atmospheric Feedback (LEAF-2) model (Walko et al. 2000) is used. This model accounts for the exchange of heat and moisture among the soil, vegetation, canopy, surface water, and atmosphere. LEAF-2 explicitly represents canopy processes based on Deardorff's (1978) "big leaf" concept. It also represents the details of turbulent exchange and radiative transfer, as well as transpiration, precipitation, and fluxes of heat and moisture between the soil or snow and the atmosphere (Lee 1992; Walko et al. 2000).

The initialization of soil moisture and soil temperature in LEAF-2 should be on the basis of observations, but these are entirely lacking over the Sydney region. We therefore initialized both soil temperature and soil moisture homogeneously over the region. We initialized soil moisture at 35% of moisture capacity in each of the 11 soil layers. The soil type was uniformly sandy clay loam. We explored the sensitivity of the simulated storm to initial soil moisture under both current and natural land cover by perturbing the initial soil moisture to 25% and 45% of moisture capacity (we did not run each factorial experiment). The impact of land cover change on the simulated storm was independent of soil moisture initialization across this initial range. Soil temperature was initialized at 2 K below the temperature of the lowest atmospheric level for the top soil layer, to 5 K warmer than the temperature of the lowest

atmospheric level for the deepest soil layer. Again, we explored the effect on our results of small perturbations in soil temperature initialization, and the simulated storm was insensitive. However, we did not explore the sensitivity of the storm to an introduction of a heterogeneous initialization of soil temperature or soil moisture.

To differentiate between land cover types in LEAF-2, various biophysical parameters need to be modified that reflect the nature of the terrestrial surface. These biophysical parameters include albedo α, leaf area index (LAI), vegetation fraction δf_m, aerodynamic roughness length z_0, zero-plane displacement height d, emissivity ε, and root depth R_d. For this study, new land surface classes were required to represent the specific land cover types found within the Sydney basin. The classes included in this study are

1) dense urban [confined to the city core and Parramatta central business district (CBD), approximately 20 km west of Sydney's CBD],
2) new urban (newly established residential suburbs lacking mature trees),
3) established urban (residential suburbs with mature trees),
4) agricultural land (incorporating all agricultural activity; in western Sydney, most agricultural land is pasture for grazing or market gardens), and
5) bushland (i.e., natural vegetation, primarily ~20-m-high trees with 40% cover).

This number and definition of land cover classes was based on previous studies of a similar nature (Sailor 1995; Brown and Williams 1998; Grimmond and Oke 1999; Brown 2000), combined with the specific nature of Sydney's land use patterns. The principal characteristics defining these classes are built versus green space, canopy height, and building density (Brown 2000). Table 3 shows the actual biophysical parameter values used and the supporting literature.

To explore the potential impact of LCC over the Sydney region, high-resolution land cover datasets describing the Sydney basin's current land use patterns and the land cover prior to European settlement were needed. The land use prior to European settlement in 1788 is not known at the level of spatial detail required by RAMS. We therefore assume that the region was homogeneously covered by native bush, primarily 20-m eucalypt forest. This vegetation still covers some areas of the Sydney region. The current land use datasets were generated by GIS classification techniques from Landsat Thematic Mapper (TM) satellite imagery and were incorporated into LEAF-2. Classification of heterogeneous urban areas from remotely sensed imagery

TABLE 3. Classes added to LEAF-2 and their corresponding biophysical parameter values.

Biophysical parameters	Dense urban	New urban	Established urban	Bushland	Agricultural land
α	0.16 (Brest 1987; Seaman et al. 1989; Sailor 1995; Strugnell et al. 2001)	0.17 (Brest 1987; Seaman et al. 1989; Sailor 1995; Strugnell et al. 2001)	0.135 (Brest 1987; Seaman et al. 1989; Sailor 1995; Strugnell et al. 2001)	0.14 (Collins and Avissar 1994; Sailor 1995; Pielke 2002)	0.2 (Oke 1973; Rosenberg 1974; Noilhan and Planton 1989; Seaman et al. 1989)
z_0 and d (m)	2.5, 16.7 (Grimmond and Oke 1999; Sailor 1995)	0.35, 2.4 (Grimmond and Oke 1999; Sailor 1995)	0.5, 3.3 (Grimmond and Oke 1999; Sailor 1995)	2.21, 11.34 (Seaman et al. 1989; Rozoff et al. 2003)	0.04, 0.7 (Sailor 1995; default LEAF-2 values)
LAI	3.8 (Sailor 1995; Rozoff et al. 2003)	2 (Sailor 1995; Rozoff et al. 2003)	4 (Sailor 1995; Rozoff et al. 2003)	4 (Sailor 1995; default LEAF-2 values)	5 (default LEAF-2 values)
δf_m (%)	0.05 (Sailor 1995; Rozoff et al. 2003)	0.05 (Sailor 1995; Rozoff et al. 2003)	0.3 (Sailor 1995; Rozoff et al. 2003)	0.4 (Sailor 1995; default LEAF-2 values)	0.85 (default LEAF-2 values)
ε (%)	0.9 (default LEAF-2 urban value)	0.9 (default LEAF-2 urban value)	0.88 (default LEAF-2 urban value)	0.86 (default LEAF-2 value)	0.95 (default LEAF-2 value)
R_d (m)	0.6	0.6	0.6	0.6	0.6

is a difficult task because of the challenges in differentiating urban areas from other land use types (Treitz et al. 1992; Gao and Skillcorn 1998; Zha et al. 2003). However, it is recognized to be a valuable tool in realistically investigating land surface impacts on meteorological processes (Dupont et al. 2004). For the purpose of this study, images from the *Landsat 7* Enhanced Thematic Mapper Plus (ETM+) were used. ETM+ includes bands in the visible, near infrared, midinfrared, and thermal infrared (Haack 1983). Six bands (excluding thermal infrared) were included when classifying the land surface. Supervised classification was performed in which representative areas of land use are selected to classify an image on the original multispectral image (Maunsel et al. 1990). The resulting land cover datasets, for the present day, are qualitatively similar to other sources of data such as air photographs, maps, and anecdotal evidence. However, we have not systematically assessed the current land cover used in RAMS with field observations.

The method to test the effect of land cover on this particular storm involved simulating the storm with the control (natural) land cover, followed by simulating the same event (using identical boundary conditions and model configuration) with current land cover. This experimental design (i.e., using identical boundary conditions and altering the land surface) follows Sailor (1995), Pielke et al. (1999), and Eastman et al. (2001) in testing model sensitivity to the land surface. Thus, using identical boundary conditions and model configuration, the changed land cover allows the influence of the land surface on the behavior of the storm to be examined. If we had run a single realization of natural land cover and a single realization of current land cover there would be a high risk that the results we obtained could be because of internal model variability. We therefore also use a factorial approach based on Henderson-Sellers (1993) and Rivers and Lynch (2004) to explore the impact of LCC on the simulated storm. The factorial approach has two advantages. First, it can reveal the significance of each individual land cover type and the potential interactions existing between each type. Second, it highlights the consistency of results. If results from the simulations are inconsistent (e.g., a range of storms occurring in different locations), it suggests a nondeterministic outcome. If a small number of types of results are obtained (e.g., storms are in one location or do not occur at all), it builds confidence that there is an association between the perturbation and the simulated results. We used a two-level full factorial experiment with the parameters (or factors) being the four current land cover classes of interest: dense urban, new urban, established urban, and agriculture. The full mode of factorial assessment was selected, and all 16 possible runs were performed (see Table 4).

3. Results and discussion

Figure 3 shows results from the natural versus current land cover simulation for a single storm. Shown is the simulated wind field over the finest grid (grid 4) for natural vegetation (first column of panels) and for current vegetation (middle column of panels). Also shown is the difference between the two (right column of panels). The shaded region in the first difference panel (top-right) shows areas where land cover was changed (see Fig. 2 for details). There are no differences in the initialization of the two storms or in the boundary conditions, and the difference plot shows no differences between the resulting simulations. At 1345 LST the natural and current simulations are similar, but a careful examination shows that the sea breeze under current vegetation propagates farther inland (see also 1400 LST).

At 1415 LST, a storm is initiated under current land cover, close to Sydney's dense CBD (Fig. 2). This storm quickly intensifies, growing to 26 km in diameter with a precipitation rate of 70 mm h^{-1}. At 1430 LST, two separate intense regions are discernable, and during the following two time steps the storm splits to form two distinct and still intense (i.e., 60–70 mm h^{-1}) storm cells, with the northern cell moving directly over Syd-

TABLE 4. Design matrix for factorial assessment (AG: agriculture, DU: dense urban, NU: new urban, EU: established urban, and B: bushland). The areas of each type in the current land cover experiment (header row) are shown in Fig. 2. Simulations that generated/did not generate storms are indicated in the second column.

	Storm (S) vs no storm (NS)	Agriculture	Dense urban	New urban	Established urban
Run 1	NS	B	DU	NU	EU
Run 2	NS	B	B	NU	EU
Run 3	NS	B	B	B	EU
Run 4	S	AG	B	B	B
Run 5	NS	B	DU	B	B
Run 6	NS	B	B	NU	B
Run 7	S	AG	DU	B	B
Run 8	S	AG	DU	NU	B
Run 9	S	AG	DU	B	EU
Run 10	NS	B	DU	B	EU
Run 11	S	AG	B	B	EU
Run 12	S	AG	B	NU	B
Run 13	S	AG	B	NU	EU
Run 14	NS	B	DU	NU	B
Run 15	S	AG	DU	NU	EU
Run 16	NS	B	B	B	B

ney's CBD. These cells move off the coast because of the westerly winds at a height of 2–4 km. At 1430 LST, the arrival of a weak precipitation feature can be seen for both land cover regimes. However, particular attention is drawn to the left column of Fig. 3, which shows a complete absence of isolated convective storm for the natural land cover simulation with the sea breeze dominating the meteorological features of the basin until the arrival of the weak precipitation feature.

A reasonable assumption would be that the existence of the dense and new urban surfaces coincident with the storm was the key factor in explaining the presence of the storm under current land cover. To explore this possible cause for the presence of the storm under current land cover, factorial experiments were conducted that capture all of the possible combinations of land cover change imposed in the change from natural to current land cover. Land cover classes (Table 3) were reverted to natural land cover (i.e., bushland) following the factorial design matrix shown in Table 4. For example, in run 1, the area of agriculture represented in the current land cover experiment is returned to bushland, as in the natural land cover experiment. In run 2, both the agricultural land and dense urban areas are returned to bushland (see Table 4 for full details).

Figure 4 shows the time step at which maximum precipitation was recorded in each factorial simulation. Some simulations produce a storm (runs 4, 7, 8, 9, 11, 12, and 13; herein referred to as storm runs) that each individually look very similar to the simulation with current land cover (top left panel of Fig. 4). All other simulations produce no precipitation (runs 1, 2, 3, 5, 6, 10, and 14; herein referred to as nonstorm runs) and are similar to the simulation with natural vegetation. Thus, the simulations fall into two groups: those that are very similar to the current land cover simulation and those that are very similar to the natural land cover simulation. There are no other results: the storm is never displaced, nor is it very much weakened or strengthened. In effect, the storm is either "on" or "off" with no solution in between.

The results shown in Fig. 4 are unambiguous in terms of the pattern of land cover used to simulate the two possible outcomes. Every simulation that includes the agricultural land over southwestern Sydney generates a storm; every simulation that omits the agricultural land fails to simulate the storm. Indeed, the presence or absence of agricultural land is the only feature within the factorial experiments that the storm runs have in common. This is not what we expected when we attempted to explain our initial results of LCC generating a storm over the urban surfaces of Sydney, and we clearly need to explain the link between the LCC over the agricultural land with the generation of a storm 10–20 km east of this area.

Convective cell intensification occurs for the storm runs by three concurrent mechanisms (relating to horizontal winds, temperature, and vertical velocity, discussed later) driven by prestorm horizontal divergence and convergence patterns associated with the sea-breeze front. Figure 5 shows horizontal divergence at 850 hPa (~1500 m) and wind vectors in the region of storm initiation (prior to storm outbreak, i.e., between 1000 and 1300 LST) for the factorial and the current land cover run. For the nonstorm runs, a relatively uniform pattern is seen whereby the divergence field stretches in a southwest-to-northeast direction, marking the return flow of the sea-breeze front (i.e., there is very little along-frontal variability, with a smooth line extending across the domain from the northeast to the southwest). The horizontal divergence pattern for the storm runs shows a disjunction in the uniform divergence pattern around 34.1°S, 150.9°E, denoting the existence of the heterogeneous landscape pattern below (the smoothness of the divergence pattern is perturbed). This difference in divergence pattern is due to the smooth agricultural land exerting less drag on the atmosphere and allowing faster surface wind speeds in comparison with the rough bush (Table 3). This condition generates a horizontal divergence pattern higher in the atmosphere that acts as a trigger to initiate the storm. Figure 6 shows a vertical cross section (at 33.95°S) across grid 4 with agricultural land on the left and dense urban areas on the right. The difference in horizontal wind speed is shown and an acceleration in the near-surface winds over the smoother agricultural land is apparent, propagating to about 1000 m. At higher altitude (between 1500 and 3000 m), the atmosphere decelerates, but only above the agricultural land.

A term closely coupled to horizontal divergence and convergence is vorticity [a measure of the rotation of a fluid (Holton 2004)], which is useful in the examination of cyclonic systems. Vorticity is frequently assessed in storm studies, including those focusing on the role of sea breezes in storm initiation (see Rotunno et al. 1988; Wilson and Megenhardt 1997; Dailey and Fovell 1999), because convergent surface flow associated with sea-breeze fronts tends to result in concentrated vorticity (Holton 2004). Figure 7 shows prestorm vorticity at 850 hPa (surface winds are also shown). Again, the pattern is unambiguous. For every storm run, the vorticity field is stronger with more variable values over the agricultural areas (negative vorticity in the Southern Hemisphere denotes cyclonic vorticity). The vorticity pattern at 850 hPa is also closely aligned to the precise location

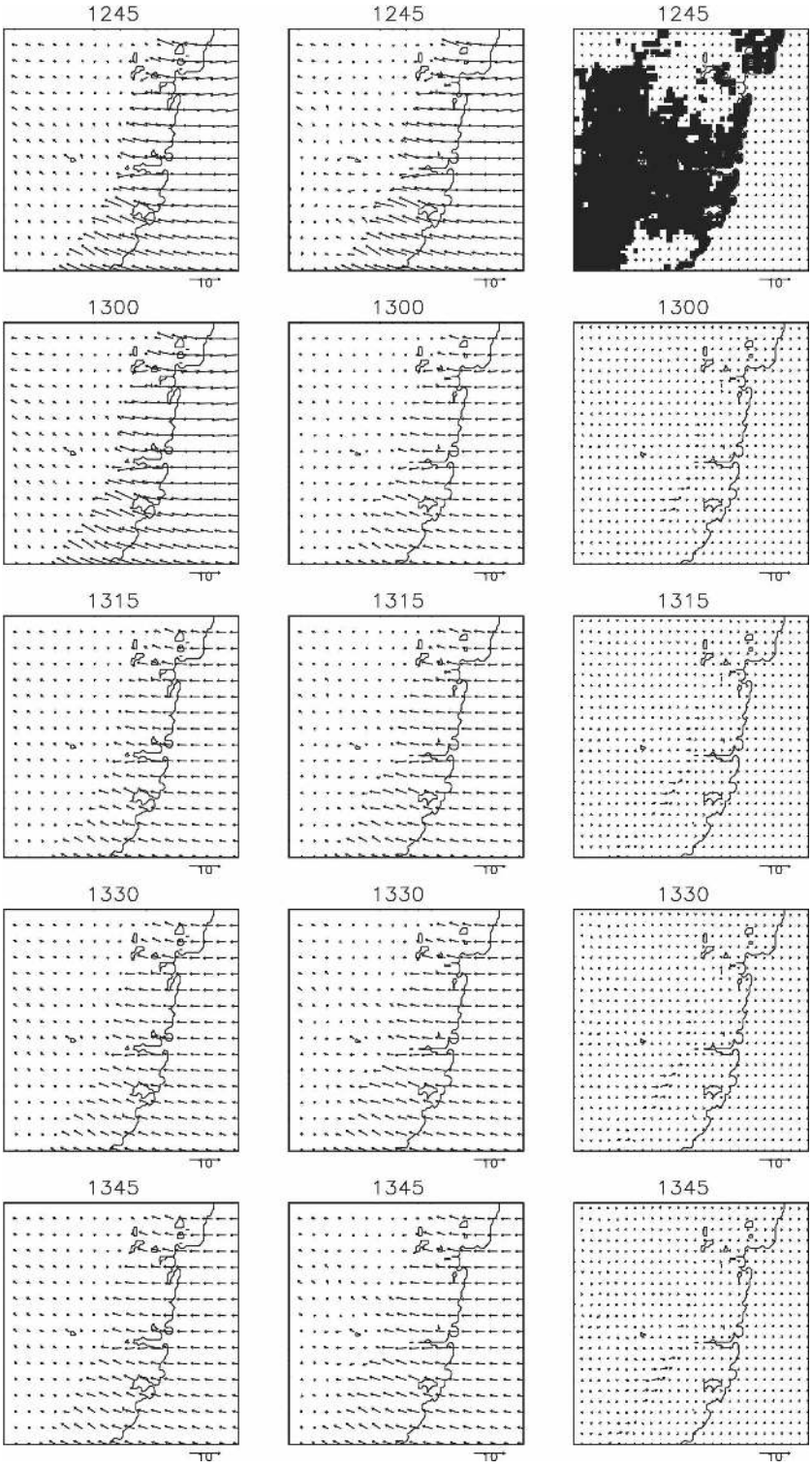

FIG. 3. Simulated storm showing precipitation rate (gray shades; mm h^{-1}) and surface winds (arrowed vectors; m s^{-1}) with (left) natural and (middle) current land cover conditions, and (right) difference (current − natural). In the top-right panel, the area of land cover change is shown for reference. Rows are the 15-min time intervals of outputs, with local standard time shown above each plot. Results are taken from the fine grid (grid 4).

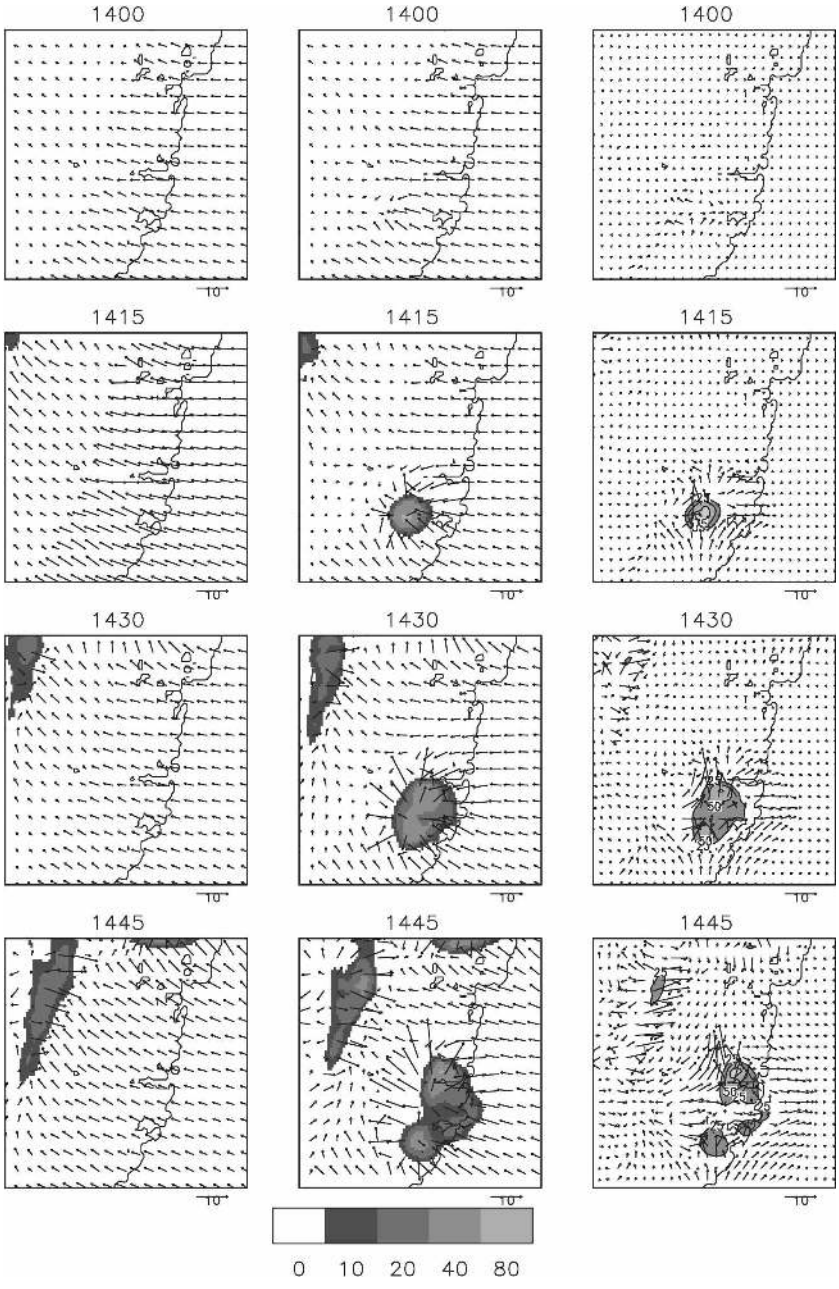

FIG. 3. (*Continued*)

of the return flow of the sea breeze, which in turn is associated with the nature of the underlying surface. Local vorticity maxima are located at the convergence zone associated with the sea-breeze front and are linked to the speed of the flow both at the surface and higher in the atmosphere. The location of storm initiation consequently coincides with local vorticity maxima and the convergence zone at the sea-breeze front where propagation has advanced the farthest inland.

At an altitude of around 1600 m, horizontal winds weaken by up to 2 m s^{-1}, temperature increases by up to 1.6°C, and vertical velocity increases by up to 2 m s^{-1}, providing positive feedbacks for storm growth through the low surface pressure these mechanisms induce. The updrafts feed warm, moist surface air into the convective cell, allowing surface convergence to intensify. The difference with all nonstorm runs is that at no stage do surface winds weaken or depart from their consistent easterly direction, temperatures are consistent, and the weak convective cell does not intensify.

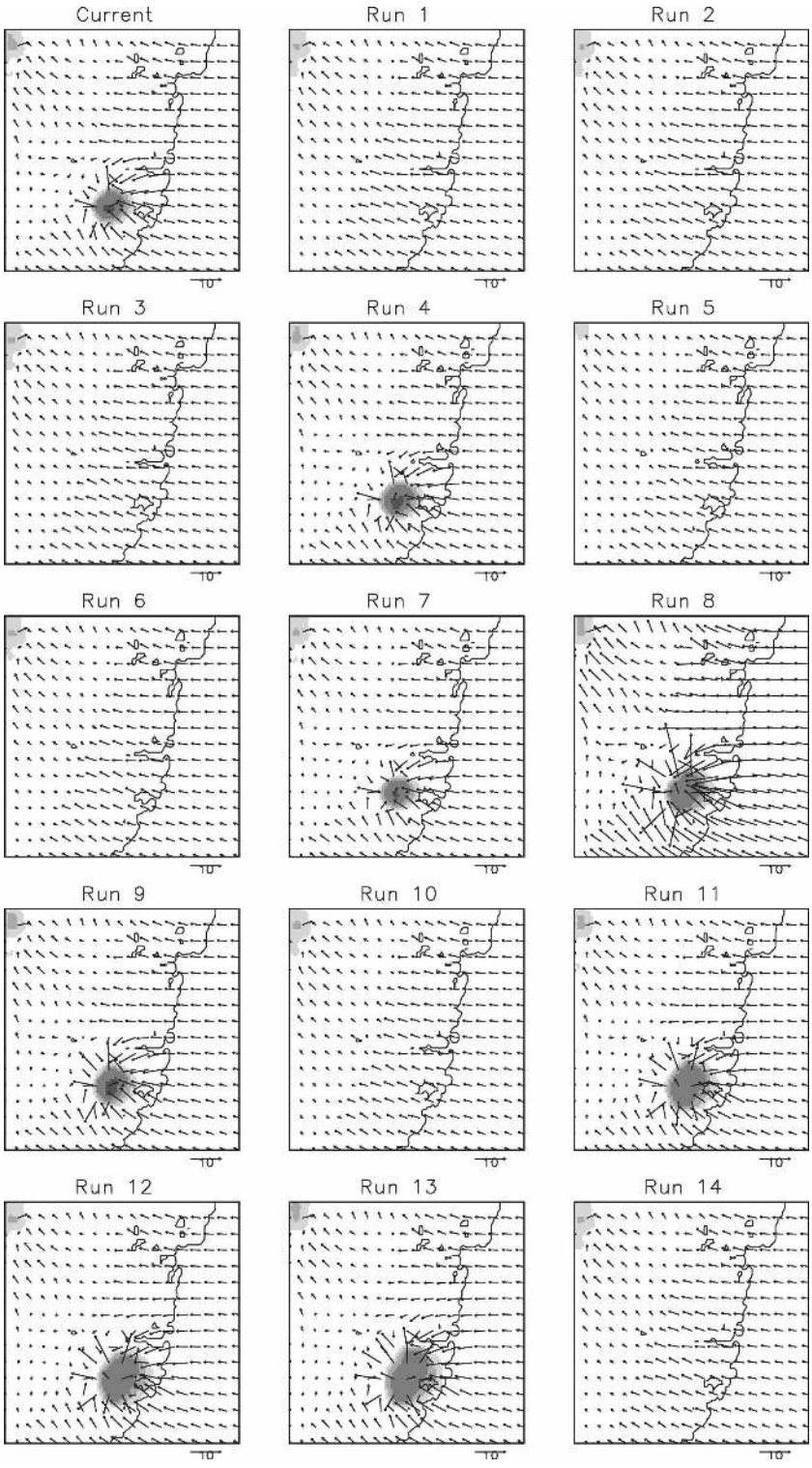

FIG. 4. Factorial simulations showing the development of the storm with precipitation rate (mm h^{-1}) and surface winds (arrowed vectors; m s^{-1}, with scale of 10 m s^{-1}) at 1415 LST. "Current" is shown for reference in the top-left panel. Run 16 is not shown because it is the natural land cover simulation shown in Fig. 3.

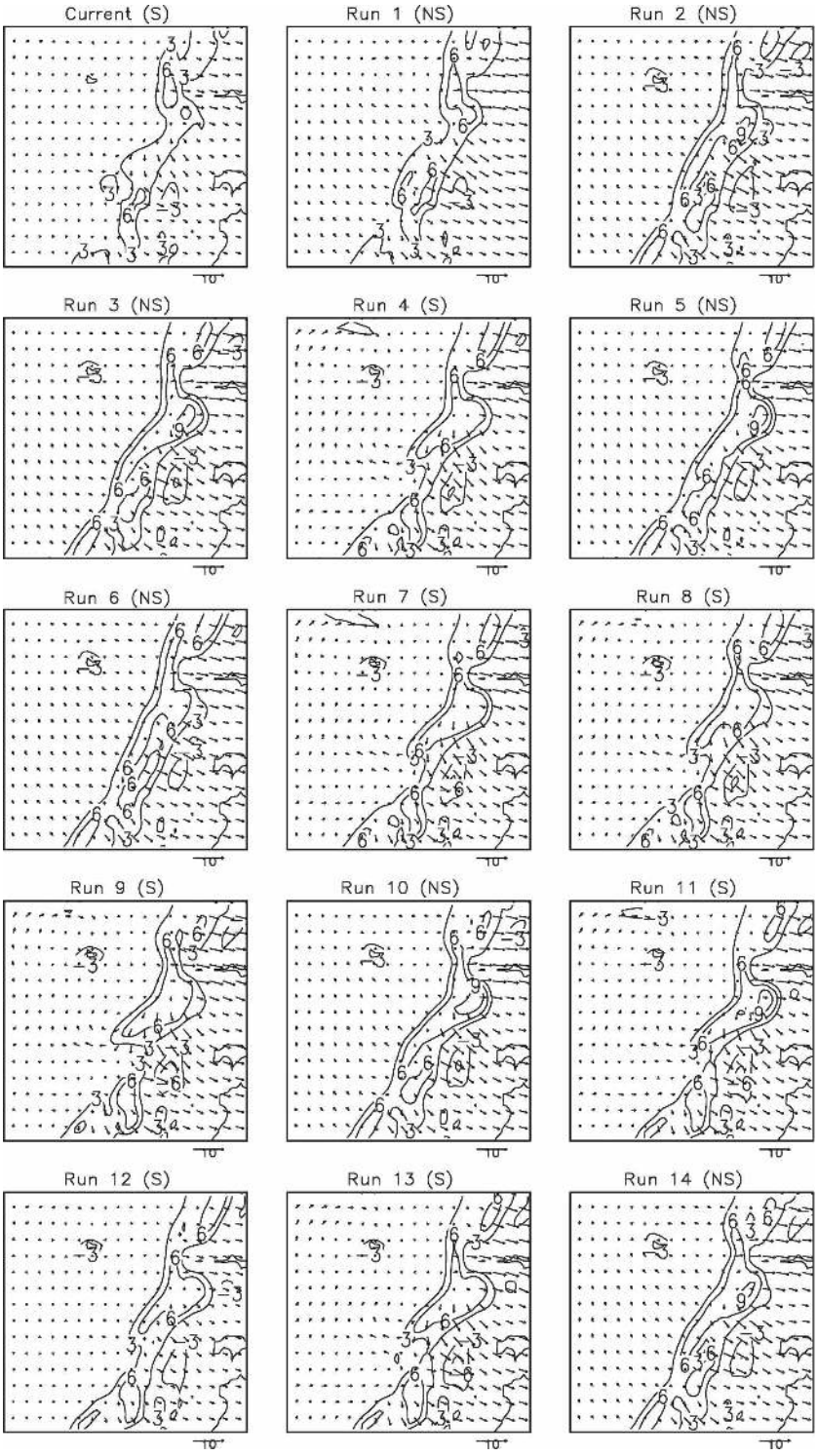

FIG. 5. Horizontal divergence (s^{-1}) and winds at 850 hPa prior to the storm for the factorial runs, with the current land cover simulation shown for reference in the top-left panel. Note that values are multiplied by 10^4 to aid clarity. Labels S and NS denote storm and no storm, respectively, from Fig. 4.

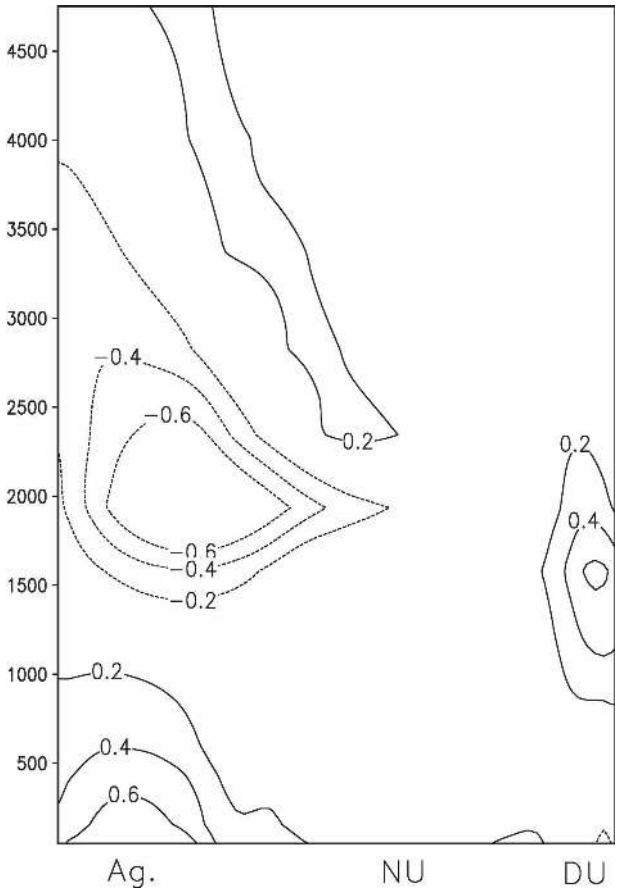

FIG. 6. Vertical cross section along 33.95°S showing the difference in wind speed (current − natural; m s^{-1}). Here, Ag is agriculture, NU is new urban, and DU is dense urban. Note the faster surface winds over agriculture by up to 0.6 m s^{-1}.

Furthermore, in the west of the domain the sea-breeze front is more visible for runs that lack agricultural land (i.e., nonstorm runs), because in the runs with agricultural land included the smoother surface permits unobstructed flow. This is directly related to horizontal divergence and moisture convergence, which effectively provide the explanation for the development of the storm.

Note that we explored a suite of other possible reasons for the relationship between the land cover change and the storm. Figure 8 shows the impact of land cover change on the simulation of the latent heat flux averaged from 1000 to 1300 LST. Only runs 9 and 10 are shown because the simulated flux for all storm runs is very similar to that in Fig. 8a and that for all nonstorm runs is very similar to what is shown in Fig. 8b. The introduction of the agricultural area reduces the latent heat flux by 20–40 W m^{-2}, and the sensible heat flux is increased by ~100 W m^{-2} (Fig. 9). This change is possible because of a change in the net radiation related to the albedo, which is higher over the agricultural land than over the natural bush. The reduction in the latent heat flux under crops may seem counterintuitive, but irrigation is limited in this region (and is not parameterized in the model). The lower albedo of the natural vegetation, coupled with the higher roughness length, supports a higher latent heat flux; hence, when it is replaced by nonirrigated crops the latent heat flux is reduced. The change in the partitioning of the available energy affects temperature (Fig. 10), which is about 0.5°C warmer over the agricultural land. Although the change in land cover and the resulting changes in the partitioning of available energy and temperature provide a possible explanation for the changed behavior of the storm through the impact on the depth of the boundary layer [which can initiate convection (Wilson et al. 1997)], this is not the case in our simulation of the storm. However, the changes in temperature and the turbulent energy fluxes may be sufficient to affect other aspects of the meteorological conditions over Sydney that are not apparent on this day.

To demonstrate that roughness length over the agricultural land explains the behavior of this specific storm, we performed additional sensitivity tests. We modified the roughness length of the agricultural land from 0.04 m (Table 3) for run 4 (storm) to 0.03 and 0.05 m. The simulation using 0.03 m produces an identical storm to that of run 4, but the simulation using 0.05 m (and higher) did not generate a storm. There is therefore a threshold associated with the impact of the roughness length on the regional meteorological behavior in the case of this specific storm. We did not explore this further because this threshold is not a fundamental property of the system—it will be dependent on the particular meteorological conditions and initialization of this day, and it is possible that interactions between roughness length and other modeled quantities would change the sensitivity to roughness under different conditions. What is important is that the perturbation to the regional roughness length field imposed by a change in roughness length from 2.21 (bushland) to 0.04 (agricultural land) m is enough to trigger the system to exceed the threshold on this day in the model. It is clearly important to explore the nature of this threshold further for observed storms in the Sydney basin and elsewhere.

4. Summary and conclusions

This study has examined the impact of land cover change on a single storm event in the Sydney basin. A numerical model (RAMS) was run at high resolution (1 km) over the Sydney basin driven by boundary conditions from the NCEP–NCAR reanalysis. Four nested

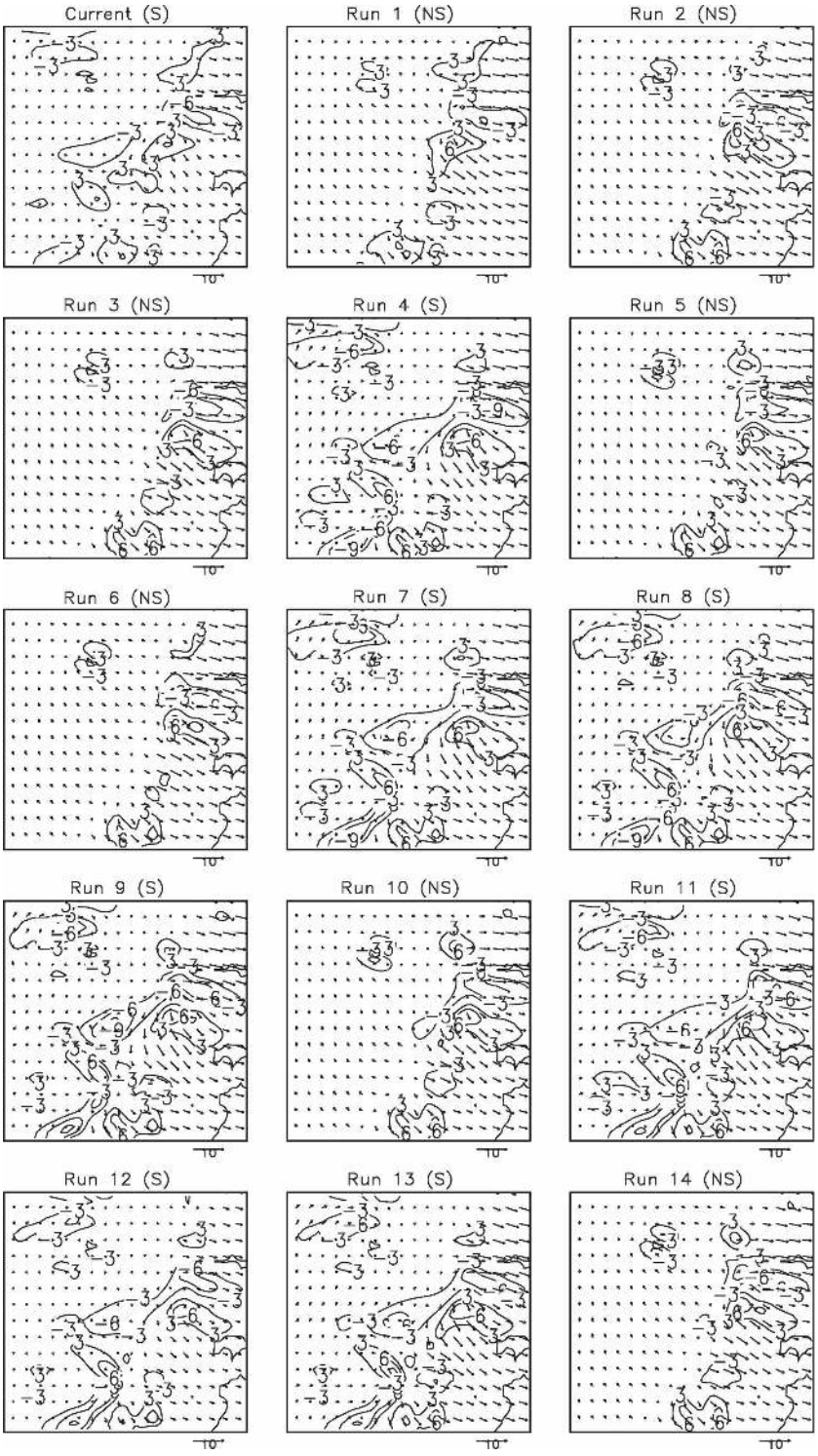

FIG. 7. Vorticity (s^{-1}) and winds at 850 hPa prior to the storm for factorial runs, with the current land cover simulation shown for reference in the top-left panel. Note that values are multiplied by 10^4 to aid clarity. Labels S and NS denote storm and no storm, respectively, from Fig. 4.

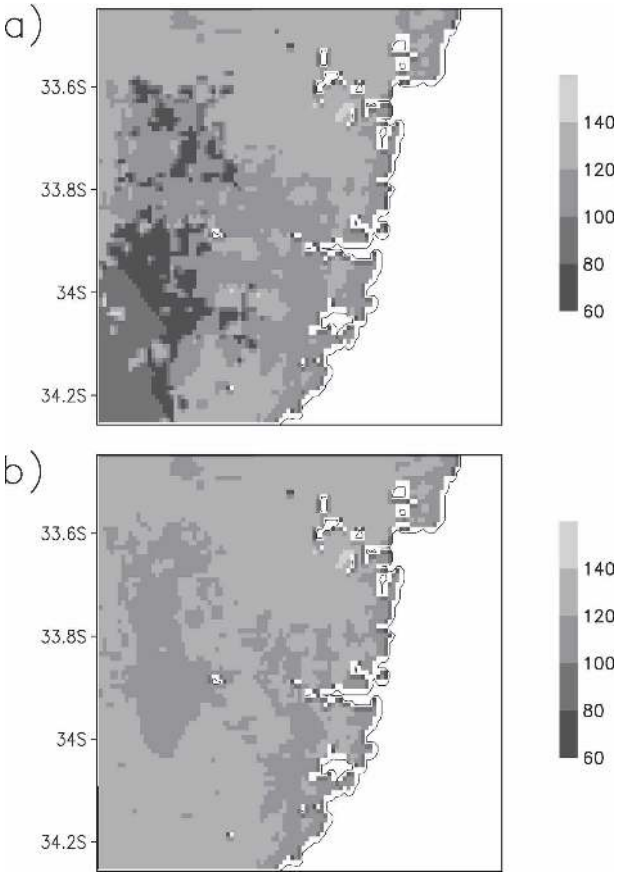

FIG. 8. Averaged (1000–1300 LST) prestorm latent heat fluxes (W m^{-2}) for runs (a) 9 and (b) 10.

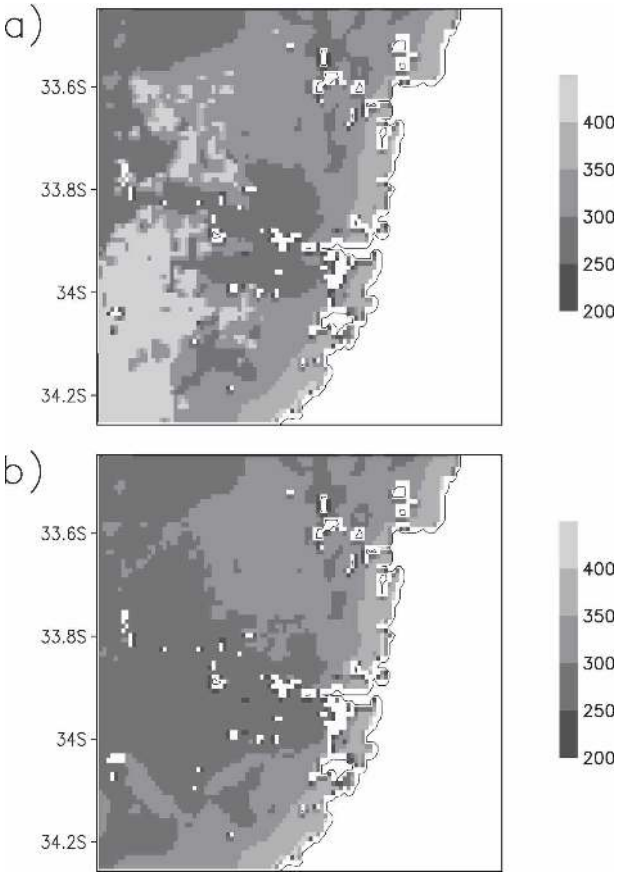

FIG. 9. Averaged (1000–1300 LST) prestorm sensible heat fluxes (W m^{-2}) for runs (a) 9 and (b) 10.

grids were used to downscale to the Sydney basin. The model used parameterization schemes implemented in previous studies with similar scope. The surface was modified within the model from natural conditions to a satellite-derived current land cover distribution, and biophysical parameters selected to represent these land cover types were based on the particular nature of Sydney's surface in conjunction with values used in previous studies.

In this case study we found that a storm simulated in close proximity to the dense urban area of Sydney's CBD using current land cover was entirely absent under natural land cover. We explored in detail the reasons for this difference using a factorial design. We showed that the presence of the agricultural land in the western region of the Sydney basin initiated processes that led to the occurrence of the storm. When this region was returned to bushland the storm was not simulated. All other possible variations in land cover contributed no explanation to the presence/absence of the storm; the dense or new urban areas specifically did not cause the storm.

The presence of the agricultural land leads to the development of a storm remote from this area because agricultural land is aerodynamically very much smoother than any other type of land cover in the Sydney basin. The smoothness of the agricultural land permits a relative acceleration of the atmosphere in comparison with the aerodynamically rough bushland. If we increase the roughness length over the agricultural area to that of bushland, the storm does not develop. The acceleration of the atmosphere perturbs the mesoscale dynamics sufficiently to affect the advancement of the sea breeze as well as modifying the local-scale vertical structure of the atmosphere, which promotes the buildup of instability. The factorial experiments also highlighted a perturbation to the horizontal divergence field associated with the area of agriculture that explains whether a storm is triggered.

This study has several limitations that should be addressed in future work. The inclusion of observational data for boundary conditions rather than NCEP–NCAR boundary conditions is one priority for future work. Such an inclusion would enable a direct simulation of

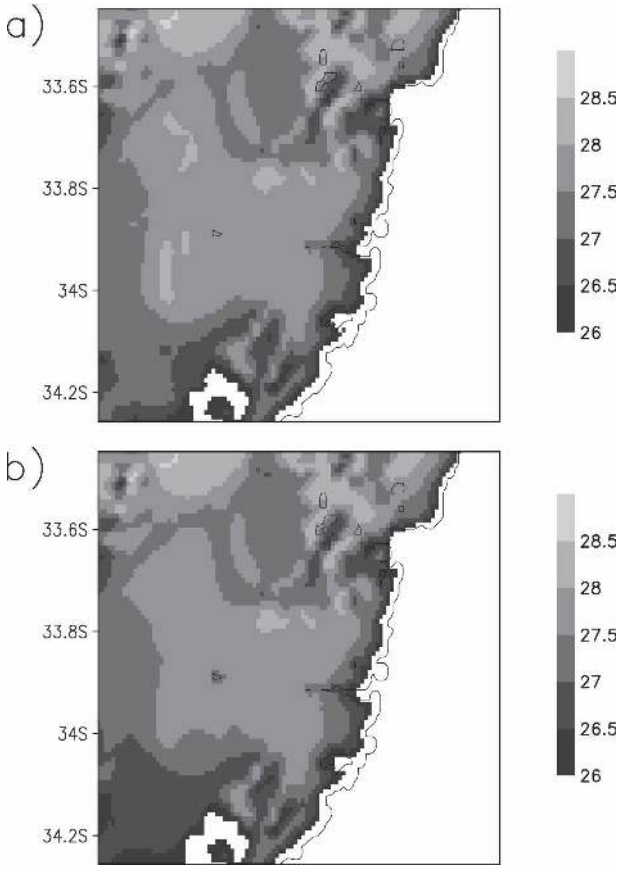

FIG. 10. Averaged (1000–1300 LST) prestorm temperatures (°C) for runs (a) 9 and (b) 10.

observed storms. Assessing the robustness of the model configuration is also important to improve the accuracy of the simulations. It is also recognized that this study presents only one storm. Previous work has indicated a nonsystematic result among different storm types in which LCC ranges from having minimal influence through to the impact presented in this paper (see Gero et al. 2006). The results in this paper are not "typical"—we have no evidence that the presence of the agriculture in southwestern Sydney has affected the climatological characteristics of storms over the Sydney urban core, or that replacing the agricultural area with urban surfaces would have a statistically robust impact on any storm climatological description. However, we do show that there is now modeling evidence to suggest that Sydney may be affected by complex urban land use–weather feedbacks in similar ways to other large coastal cities overseas (see Shepherd 2005) and that further investigation of these feedbacks over Sydney would be worthwhile.

Despite there being no evidence that the results in this paper demonstrate a systematic impact of the land cover on storms (this is a single case study), it does not mean that the results are not useful. Our results suggest that groups developing parameterizations of urban surfaces for forecasting or climate-change projection need to consider all types of nonnatural surfaces, given that our results indicate that it was LCC at the periphery of the urban surface that was significant in explaining this particular storm. If we were trying to forecast this storm, the observed land cover would be a prerequisite. For this storm, the roughness-length field was the key parameter, but the impact of specific land cover types on the latent and sensible heat fluxes points to an atmospheric forcing term that may be important to include in other meteorological conditions.

Our results also offer a warning to all of us working in mesoscale modeling. The results shown in Fig. 3 are "perfect" in that we appeared to find a causal relationship between the urban surface and storms. It would have been attractive to accept this result and to argue a cause-and-effect relationship between the building of cities and the intensification of storms. In our case study, such an argument would have been fundamentally misleading, as demonstrated by the factorial experiments. This result strongly points to the need to explore either multiple examples or to use factorial or ensemble methods when exploring the impact of LCC on meteorological behavior. To be specific, a single simulation of "before" and a single simulation of "after" an LCC is extremely limiting and is potentially misleading.

In conclusion, our results demonstrate an impact of agricultural land on a storm that forms over Sydney's new and dense urban areas. The mechanisms that link the smooth agricultural land to mesoscale atmospheric processes are consistent across all of our experiments. This result strongly suggests that the changes in the mesoscale circulations that trigger this single storm are likely to exist in other case studies and that the nature of the land cover over the Sydney basin does affect the regional meteorological behavior because it perturbs a particularly important component of that meteorological behavior (the sea breeze). Implications of this research also extend to the insurance industry. The most expensive insured event of Australia's history was the Sydney hailstorm of April 1999. The clear impact of LCC on one Sydney storm at least points to a need for a more systematic assessment of the relationship between land cover and climate. There is the possibility that further urban development might change (increase or decrease) the exposure of the insurance industry to weather-related risk.

Given that many major cities are coastal and that land clearing for agriculture farther inland from the city

is common, we suspect that the results described in this paper would be common in many areas. Our results suggest that groups forecasting the meteorological behavior of these areas need to consider the changing nature of the land surface when attempting to improve forecast models.

Acknowledgments. The authors thank Carol Jacobson for her assistance with the land cover datasets. We also thank Professor Roger Pielke Sr. for his support of our use of RAMS. Doctors Bart Geerts and Gemma Narisma provided valuable advice and suggestions on this paper.

REFERENCES

Aikman, F., III, J. G. W. Kelley, J. T. McQueen, T. F. Gross, and G. Szilagyi, 2000: Atmospheric and oceanographic analyses and forecasts for the Chesapeake Bay region during the Coastal Marine Demonstration Project. *Proc. Fifth Symp. on Integrated Observing Systems,* Alberqurque, NM, Amer. Meteor. Soc., CD-ROM, 2.3.

Arnfield, A. J., 2003: Two decades of urban climate research: A review of turbulence, exchanges of energy and water, and the urban heat island. *Int. J. Climatol.,* **23,** 1–26.

Atkinson, B. W., 1971: The effect of an urban area on the precipitation from a moving thunderstorm. *J. Appl. Meteor.,* **10,** 47–55.

Avissar, R., and R. A. Pielke, 1989: A parameterization of heterogeneous land surfaces for atmospheric numerical models and its impact on regional meteorology. *Mon. Wea. Rev.,* **117,** 2113–2136.

——, C. P. Weaver, D. Werth, R. A. Pielke, R. Rabin, A. J. Pitman, and M. A. Silva-Dias, 2004: The regional climate in Kabat. *Vegetation, Water, Humans and the Climate*, P. M. Claussen et al., Eds., Springer-Verlag, 21–32.

Baik, J. J., Y.-K. Kim, and H. Y. Chun, 2001: Dry and moist convection forced by an urban heat island. *J. Appl. Meteor.,* **40,** 1462–1474.

Balling, R. C., and S. W. Brazel, 1987: Recent changes in Phoenix, Arizona, summertime diurnal precipitation patterns. *Theor. Appl. Climatol.,* **38,** 50–54.

Beljaars, A. C. M., P. Viterbo, and M. J. Miller, 1996: The anomalous rainfall over the United States during July 1993: Sensitivity to land surface parameterization and soil moisture anomalies. *Mon. Wea. Rev.,* **124,** 362–383.

Betts, A. K., J. H. Ball, A. C. M. Beljaars, M. J. Miller, and P. A. Viterbo, 1996: The land surface–atmosphere interaction: A review based on observational and global modeling perspectives. *J. Geophys. Res.,* **101,** 7209–7225.

Bornstein, R., and Q. Lin, 2000: Urban heat islands and summertime convective thunderstorms in Atlanta: Three case studies. *Atmos. Environ.,* **34,** 507–516.

Brest, C., 1987: Seasonal albedo of an urban/rural landscape from satellite observations. *J. Climate Appl. Meteor.,* **26,** 1169–1187.

Brown, M. J., 2000: Urban parameterizations for mesoscale meteorological models. *Mesoscale Atmospheric Dispersion,* Z. Boybeyi, Ed., Wit Press, 193–255.

——, and M. D. Williams, 1998: An urban canopy parameterization for mesoscale models. *Proc. of the Second Urban Symp.,* Albuquerque, NM, Amer. Meteor. Soc., 144–147.

Bureau of Meteorology, 1993: Report on the Sydney hailstorm, March 1990. Bureau of Meteorology Phenomena Rep. F2.16, 44 pp.

——, 1995: The 21st January 1991 Sydney severe thunderstorm. Bureau of Meteorology Phenomena Rep. F2.17, 26 pp.

Castro, C. L., R. A. Pielke, and G. E. Liston, 2001: Simulation of the North American monsoon in different Pacific SST regimes using RAMS. *Proc. 26th Annual Climate Diagnostics and Prediction Workshop*, La Jolla, CA, NOAA. [Available online at http://www.cpc.ncep.noaa.gov/products/proceedings/cdw_proceedings/Castro.pdf.]

Changnon, S. A., 1968: The La Porte weather anomaly—Fact or fiction? *Bull. Amer. Meteor. Soc.,* **49,** 4–11.

Collins, D. C., and R. Avissar, 1994: An evaluation with the Fourier amplitude sensitivity test (FAST) of which land surface parameters are of greatest importance in atmospheric modeling. *J. Climate,* **7,** 681–703.

Copeland, J. H., R. A. Pielke, and T. G. F. Kittel, 1996: Potential climatic impacts of vegetative change: A regional modeling study. *J. Geophys. Res.,* **101,** 7409–7418.

Cotton, W. R., J. F. Weaver, and B. A. Beitler, 1995: An unusual summertime downslope wind event in Fort Collins, Colorado, on 3 July 1993. *Wea. Forecasting,* **10,** 786–797.

——, and Coauthors, 2003: RAMS 2001: Current status and future directions. *Meteor. Atmos. Phys.,* **82,** 5–29.

Dailey, P. S., and R. G. Fovell, 1999: Numerical simulation of the interaction between the sea breeze front and horizontal convective rolls. Part I: Offshore ambient flow. *Mon. Wea. Rev.,* **127,** 858–878.

Deardorff, J. W., 1978: Efficient production of ground surface temperature and moisture with the inclusion of a layer of vegetation. *J. Geophys. Res.,* **83,** 1889–1903.

Denis, B., R. Laprise, and D. Caya, 2003: Sensitivity of a regional climate model to the resolution of the lateral boundary conditions. *Climate Dyn.,* **20,** 107–126.

Dupont, S., J. Ching, and S. Burian, 2004: Introduction of urban canopy parameterization into MM5 to simulate urban meteorology at neighborhood scale. Preprints, *Symp. on Planning, Nowcasting, and Forecasting in the Urban Zone,* Seattle, WA, Amer. Meteor. Soc., paper 4.4.

Eastman, J. L., M. B. Coughenhour, and R. A. Pielke, 2001: Does grazing affect regional climate? *J. Hydrometeor.,* **2,** 243–253.

Environment Protection Authority, New South Wales, 2003: State of the environment report 2003. [Available online at http://www.epa.nsw.gov.au/soe/soe2003/.]

Gao, J., and D. Skillcorn, 1998: Capability of SPOT XS data in producing detailed land cover maps at the urban rural periphery. *Int. J. Remote Sens.,* **19,** 2877–2891.

Gero, A. F., A. J. Pitman, G. T. Narisma, C. Jacobson, and R. A. Pielke, 2006: The impact of land cover change on storms in the Sydney Basin. *Global Planet. Change,* in press.

Grimmond, C., and T. R. Oke, 1999: Aerodynamic properties of urban areas derived from analysis of surface form. *J. Appl. Meteor.,* **38,** 1262–1292.

Haack, B. N., 1983: An analysis of Thematic Mapper simulator data for urban environments. *Remote Sens. Environ.,* **13,** 265–275.

Harrington, J. Y., 1997: The effects of radiative and microphysical processes on simulated warm and transition season Arctic stratus. Ph.D. dissertation, Atmospheric Science Paper 637, Colorado State University, 289 pp.

Henderson-Sellers, A., 1993: A factorial assessment of the sensitivity of the BATS land-surface parameterization scheme. *J. Climate,* **6,** 227–247.

Hjelmfelt, M. R., 1982: Numerical simulation of the effects of St. Louis on mesoscale boundary layer airflow and vertical air motion: Simulation of urban vs. non-urban effects. *J. Appl. Meteor.,* **21,** 1239–1257.

Holton, J. R., 2004: *An Introduction to Dynamic Meteorology.* 4th ed. International Geophysics Series, Vol. 88, Academic Press, 535 pp.

Holtslag, A. A. M., and M. Ek, 1995: The simulation of surface fluxes and boundary layer development over the pine forest in HAPEX-MOBILHY. *J. Appl. Meteor.,* **35,** 202–213.

Huff, F. A., 1986: Urban hydrological review. *Bull. Amer. Meteor. Soc.,* **67,** 703–712.

Jauregui, E., and E. Romales, 1996: Urban effects on convective precipitation in Mexico City. *Atmos. Environ.,* **30,** 3383–3389.

Kain, J. S., and M. Fritsch, 1993: Convective parameterization for mesoscale models: The Kain-Fritsch scheme. *The Representation of Cumulus Convection in Numerical Models, Meteor. Monogr.*, No. 24, Amer. Meteor. Soc., 165–170.

Kalnay, E., and M. Cai, 2003: Impact of urbanization and land-use change on climate. *Nature,* **423,** 528–531.

——, and Coauthors, 1996: The NCEP/NCAR 40-Year Reanalysis Project. *Bull. Amer. Meteor. Soc.,* **77,** 437–471.

Klemp, J. B., and R. B. Wilhelmson, 1978: The simulation of three dimensional convective storm dynamics. *J. Atmos. Sci.,* **35,** 1070–1096.

Koch, S. E., and C. A. Ray, 1997: Mesoanalysis of summertime convergence zones in central and eastern North Carolina. *Wea. Forecasting,* **12,** 56–77.

Kuo, H. L., 1974: Further studies of the parameterization of the influence of cumulus convection on large-scale flow. *J. Atmos. Sci.,* **31,** 1232–1240.

Landsberg, H. E., 1970: Man-made climate changes. *Science,* **170,** 1265–1274.

Lee, T. J., 1992: The impact of vegetation on the atmospheric boundary layer and convective storms. Ph.D. dissertation, Colorado State University, 137 pp.

Matthews, C., and B. Geerts, 1995: Characteristic thunderstorm distribution in the Sydney area. *Aust. Meteor. Mag.,* **44,** 127–138.

Maunsel, P. W., W. J. Kamber, and J. K. Lee, 1990: Optimum band selection for supervised classification of multispectral data. *Photogramm. Eng. Remote Sens.,* **56,** 55–60.

McQueen, J. T., and Coauthors, 1999: Development and evaluation of a non-hydrostatic atmospheric prediction system for the Chesapeake Bay region. *Proc. Third Conf. on Coastal Atmospheric and Oceanic Prediction,* New Orleans, LA, Amer. Meteor. Soc., 189–194.

Meyers, M. P., P. J. DeMott, and W. R. Cotton, 1992: New primary ice nucleation parameterizations in an explicit cloud model. *J. Appl. Meteor.,* **31,** 708–721.

Narisma, G. T., and A. J. Pitman, 2003: The impact of 200 years of land cover change on the Australian near surface climate. *J. Hydrometeor.,* **4,** 424–436.

Noilhan, J., and S. Planton, 1989: A simple parameterization of land surface processes for meteorological models. *Mon. Wea. Rev.,* **117,** 536–549.

Oke, T. R., 1973: City size and the urban heat island. *Atmos. Environ.,* **7,** 769–779.

Peel, D. R., A. J. Pitman, L. A. Hughes, and R. A. Pielke, 2005: The impact of realistic biophysical parameters for eucalyptus on the simulation of the January climate of Australia. *Environ. Model. Software,* **20,** 595–612.

Pielke, R. A., 2001: *Mesoscale Meteorological Modeling.* 2d ed. International Geophysics Series, No. 78, Academic Press, 676 pp.

——, and Coauthors, 1992: A comprehensive meteorological modeling system—RAMS. *Meteor. Atmos. Phys.,* **49,** 69–91.

——, T. J. Lee, J. H. Copeland, J. L. Eastman, C. L. Ziegler, and C. A. Finley, 1997: Use of USGS-provided data to improve weather and climate simulations. *Ecol. Appl.,* **7,** 3–21.

——, R. L. Walko, L. T. Steyaert, P. L. Vidale, G. E. Liston, W. A. Lyons, and T. N. Chase, 1999: The influence of anthropogenic landscape change on weather in south Florida. *Mon. Wea. Rev.,* **127,** 1663–1673.

Potts, R. J., T. D. Keenan, and P. T. May, 2000: Radar characteristics of storms in the Sydney area. *Mon. Wea. Rev.,* **128,** 3308–3319.

Ramanathan, V., P. J. Crutzen, J. T. Kiehl, and D. Rosenfield, 2001: Aerosols, climate and the hydrological cycle. *Science,* **294,** 2119–2124.

Rivers, A. R., and A. H. Lynch, 2004: On the influence of land cover on early Holocene climate in northern latitudes. *J. Geophys. Res.,* **109,** D21114, doi:10.1029/2003JD004213.

Rodriguez-Camino, E., and R. Avissar, 1999: Effective parameters for surface fluxes in heterogeneous terrain. *Tellus,* **51A,** 387–399.

Rosenberg, N. J., 1974: *Microclimate: The Biological Environment.* John Wiley and Sons, 315 pp.

Rosenfield, D., 1999: TRMM observed first direct evidence of smoke from forest fires inhibiting rainfall. *Geophys. Res. Lett.,* **26,** 3105–3108.

Rotunno, R., J. B. Klemp, and M. L. Weisman, 1988: A theory for strong, long-lived squall lines. *J. Atmos. Sci.,* **45,** 463–485.

Rozoff, C. M., W. R. Cotton, and J. O. Adegoke, 2003: Simulation of St. Louis, Missouri, land use impacts on thunderstorms. *J. Appl. Meteor.,* **42,** 716–738.

Sailor, D. J., 1995: Simulated urban climate response to modification in surface albedo and vegetative cover. *J. Appl. Meteor.,* **34,** 1694–1704.

Schar, C., D. Luthi, U. Beyerle, and E. Heise, 1999: The soil–precipitation feedback: A process study with a regional climate model. *J. Climate,* **12,** 722–741.

Seaman, N. L., F. F. Ludwig, E. G. Donall, T. T. Warner, and C. M. Bhumralkar, 1989: Numerical studies of urban planetary boundary layer structure under realistic synoptic conditions. *J. Appl. Meteor.,* **28,** 760–781.

Shepherd, J. M., 2005: A review of current investigations of urban-induced rainfall and recommendations for the future. *Earth Interactions,* **9**. [Available online at http://EarthInteractions.org.]

——, and S. J. Burian, 2003: Detection of urban-induced rainfall anomalies in a major coastal city. *Earth Interactions,* **7**. [Available online at http://EarthInteractions.org.]

Spillane, K. T., and B. Dixon, 1969: A severe storm radar signature in the Southern Hemisphere. *Aust. Meteor. Mag.,* **17,** 134–142.

Strugnell, N. C., W. Lucht, and C. Schaaf, 2001: A global albedo data set derived from AVHRR data for urban climate simulations. *Geophys. Res. Lett.,* **28,** 191–194.

Treitz, M., P. J. Howarth, and P. Gong, 1992: Application of satellite and GIS technologies for land cover and land use mapping at the urban rural fringe: A case study. *Photogramm. Eng. Remote Sens.,* **58,** 439–448.

Tremback, C. J., 1990: Numerical simulation of a mesoscale convective complex: Model development and numerical results. Ph.D. dissertation, Atmospheric Science Paper 465, Colorado State University, 187 pp.

Trenberth, K. E., 2004: Rural land-use change and climate. *Nature,* **427,** 213

Viterbo, P., and A. K. Betts, 1999: Impact on ECMWF forecasts of changes to the albedo of the boreal forests in the presence of snow. *J. Geophys. Res.,* **104,** 27 803–27 810.

——, A. C. M. Beljaars, J.-F. Mahfouf, and J. Teixeira, 1999: The representation of soil moisture freezing and its impact on the stable boundary layer. *Quart. J. Roy. Meteor. Soc.,* **125,** 2401–2426.

Walko, R. L., and C. J. Tremback, 2002: RAMS: Regional Atmospheric Modeling System, version 4.3/4.4—Introduction to RAMS 4.3/4.4. *ASTER Division, Mission Research, Inc., Rep., 11 pp. [Also available online at http://www.atmet.com.]

——, ——, and R. F. A. Hertenstein, 1995: RAMS: The Regional Atmospheric Modeling System, version 3b, user's guide. *ASTER Division, Mission Research, Inc., Rep., 117 pp. [Also available online at http://www.atmet.com.]

Walko, R. L., and Coauthors, 2000: Coupled atmosphere–biophysics–hydrology models for environmental modeling. *J. Appl. Meteor.,* **39,** 931–944.

Wilson, J. W., and W. E. Schreiber, 1986: Initiation of convective storms at radar-observed boundary-layer convergent lines. *Mon. Wea. Rev.,* **114,** 2516–2536.

——, and D. L. Megenhardt, 1997: Thunderstorm initiation, organization, and lifetime associated with Florida boundary layer convergence lines. *Mon. Wea. Rev.,* **125,** 1507–1525.

Zha, Y., J. Gao, and S. Ni, 2003: Use of normalised difference built-up index in automatically mapping urban areas from TM imagery. *Int. J. Remote Sens.,* **24,** 583–594.